Low-Intensity Pulsed Ultrasound Enhances Bone Formation around Miniscrew Implants

Khaliunaa Ganzorig[a], Shingo Kuroda[b], Yuichi Maeda[a], Karima Mansjur[a], Minami Sato[a], Kumiko Nagata[b], Eiji Tanaka[b]

[a]Department of Orthodontics and Dentofacial Orthopedics, Tokushima University Graduate School of Oral Sciences, Tokushima, Japan

[b]Department of Orthodontics and Dentofacial Orthopedics, Institute of Health Biosciences, Tokushima University Graduate School, Tokushima, Japan

All authors certify that they have no conflict of interest.

Correspondence to: Eiji Tanaka

Department of Orthodontics and Dentofacial Orthopedics, Institute of Health Biosciences, Tokushima University Graduate School, 3-18-15 Kuramoto-Cho, Tokushima 770-8504, Japan.

Tel: +81 88 6337357 / Fax: +81 88 6339139.

E-mail: etanaka@tokushima-u.ac.jp

Keywords: Low-intensity pulsed ultrasound, miniscrew implant, bone formation, stainless steel and titanium

ABSTRACT

Miniscrew implants (MSIs) are currently used to provide absolute anchorage in orthodontics; however, their initial stability is an issue of concern. Application of low-intensity pulsed ultrasound (LIPUS) can promote bone healing. Therefore, LIPUS application may stimulate bone formation around MSIs and enhance their initial stability. *Aim.* To investigate the effect of LIPUS exposure on bone formation after implantation of titanium (Ti) and stainless steel (SS) MSIs. *Methods.* MSIs made of Ti-6Al-4V and 316L SS were placed on rat tibiae and treated with LIPUS. The bone morphology around MSIs was evaluated by scanning electron microscopy and three-dimensional micro-computed tomography. MC3T3-E1 cells cultured on Ti and SS discs were treated with LIPUS, and the temporary expression of alkaline phosphatase (ALP) was examined. *Results*. Bone-implant contact increased gradually from day 3 to day 14 after MSI insertion. LIPUS application increased the cortical bone density, cortical bone thickness, and cortical bone rate after implantation of Ti and SS MSIs ($P < 0.05$). LIPUS exposure induced ALP upregulation in MC3T3-E1 cells at day 3 ($P < 0.05$). *Conclusion.* LIPUS enhanced bone formation around Ti and SS MSIs, enhancing the initial stability of MSIs.

1. INTRODUCTION

Anchorage control is a key component in clinical orthodontic success. Numerous anchorage devices have been proposed and used for more than a century. However, most of these devices have disadvantages, in that their effectiveness depends on patient compliance and they cannot provide absolute anchorage. The concept of skeletal anchorage was initially introduced to the orthodontic field in the 1980s, reaching worldwide acceptance by the year 2000.[1-5] In the skeletal anchorage approach, screws or miniplates are fixed directly onto the bone and provide absolute anchorage for several kinds of tooth movements.

Miniscrew implants (MSIs) made of Ti-6Al-4V alloy offer biocompatibility, improved comfort, relative noninvasiveness, and fewer limitations in placement compared to other skeletal anchorage devices.[6,7] For these reasons, MSI use is generally accepted by orthodontists and patients. However, the clinical use of MSIs has been associated with some risks and complications, particularly screw failure.[8] A recent systematic review found an overall success rate of 86.5% among 4,987 MSIs placed in 2,281 patients. This rate is significantly lower than the success rate of dental implants for prosthetic restorations.[9] Therefore, increasing the success rate of MSIs in clinical orthodontics is an urgent issue.

Low-intensity pulsed ultrasound (LIPUS) is a form of physical energy that can be delivered to living tissue as acoustic waves. Used extensively as a therapeutic, operative, and diagnostic tool in medicine, LIPUS does not have any known deleterious, carcinogenic, or thermal effects on living tissues. LIPUS is well accepted as a noninvasive and safe tool for the treatment of bone fractures.[10] In previous reports, LIPUS increased the rate of repair of bone fractures at all stages of the healing process[11–14] and increased the mechanical properties of callus.[15,16] Radical changes in density are inherent in a healing tissue, which may lead to gradients in physical strain.[17]

Ultrasound can be generated through several possible mechanisms. Microbubble compression and acoustic streaming can have direct effects on cell membrane permeability.[18] Physical force serves as an extracellular signal to various cell types, including bone cells. For example, BMP-2–induced bone formation[19] and cellular mineralization[20] were enhanced after various types of biophysical stimulation of bone cells. Additionally, ultrasound has been shown to enhance protein synthesis.[21,22]

Most MSI failures occur within a week after implant placement. This fact implies that early bone metabolism around the inserted screws might be related to the screw stability. If LIPUS can stimulate bone formation around the MSI, then LIPUS application after MSI implantation may be able to enhance the initial implant stability. Therefore, the aim of this study was to evaluate the effect of LIPUS application on bone formation after placement of MSIs made of Ti-6Al-4V alloy or stainless steel (SS).

2. MATERIAL AND METHODS

2.1. Animals

Forty 6-week-old Sprague-Dawley rats (body weight: 190.0–210.5 g) were used in this study. All animals were treated in accordance with the Guidelines for Animal Experiments at the Laboratory Animal Centre of Tokushima University. Animals were caged individually under automatically controlled conditions, with a temperature of 23 °C, humidity of 50%, and a 12 h:12 h light: dark cycle. Animals were given free access to tap water and rodent chow. All of the protocols of the study were approved by the Ethics Committee of Tokushima University.

2.2. Surgical Procedure

Each animal was anesthetized with an intra-abdominal injection of 50 mg/kg sodium pentobarbital (Kyoritsu, Tokyo, Japan). The skin was cleaned and incised with a scalpel blade. The tibia surface was exposed, and the implant site was prepared by a standard surgical technique with sharp drills. All drilling procedures were done under profuse irrigation with sterile saline. For each animal, four MSIs were inserted with a miniature jewelry screwdriver. MSIs measured 1.0 mm in inner diameter, 1.5 mm in outer diameter, and 1.6 mm in length. MSIs were made of Ti-6Al-4V or 316L SS (Nishimura Metal, Sabae, Japan).

2.3. In Vivo LIPUS Application

The LIPUS exposure system used in this study was modified from a clinical device (Osteotron-D IV; Ito Co, Tokyo, Japan) and was used in both the in vitro and in vivo experiments. Pulsed ultrasound signal was transmitted at a frequency of 1.5 MHz with a spatially averaged intensity of 30 mW/cm^2 and 1:4 pulse rate (2 ms on to 8 ms off). LIPUS exposure was initiated 24 h after MSI implantation. Tibiae on the right side were irradiated with LIPUS for 20 min/d. Tibiae on the other side served as a sham-irradiated control.

2.4. Micro-Computed Tomography (μ-CT) Analysis

Animals were perfusion-fixed with 4% paraformaldehyde (Wako, Osaka, Japan) 0, 3, 7, and 14 days after MSI implantation. The tibiae were resected and dehydrated by incubation in a graded ethanol series (70%, 80%, 90%, 99%, 100%, and 100% ethanol, v/v) for 12 h at each concentration. Tibiae were embedded in methyl methacrylate resin (Technovit 9100; Kulzer, Wehrheim, Germany). The resin blocks were scanned by μ-CT (Latheta LCT-200; Hitachi Aloka Medical, Tokyo, Japan). Images consisted of 936 slices with a voxel size of 24 μm in all three axes. Cortical

bone and MSIs in the specimens were imaged and reconstructed in three dimensions. Regions of interest adjacent to the implants were analyzed to determine the cortical bone density (CBD; mg hydroxyapatite/cm^3), cortical bone thickness (CBT; mm) and cortical bone ratio (CBR; %). CBD was defined as the volumetric density of calcium hydroxyapatite. CBR was calculated as the amount of cortical bone area divided by the total area in the tread.

2.5. Scanning Electron Microscopy (SEM) Analysis

After μ-CT analysis, the resin blocks were trimmed and prepared for analysis by SEM (Carry Scope JCM-5700; JOEL, Tokyo, Japan; Fig. 1). Acquired images were analyzed with a digital image analysis software (ImageJ version 1.44; US National Institutes of Health, Bethesda, MD).

2.6. Cell Culture

Ti-6Al-4V and 316L SS discs measuring 33 mm in diameter and 1 mm in thickness were used. These discs were perfectly fitted to the bottom of wells in six-well cell culture plates. The discs were sterilized, cleaned with ethanol and double-distilled water (ultrasonication, 15 min per wash step), and autoclaved. Newborn mouse calvaria-derived osteoblastic precursor cells (MC3T3-E1) were seeded at a density of 2×10^4 cells in growth medium containing Dulbecco's modified Eagle's medium (Invitrogen, Carlsbad, CA), 10% fetal bovine serum (JRH Biosciences, Kansas, MO), and 1% penicillin G (Meiji Seika, Tokyo, Japan). Cells were grown in an incubator at 37 °C and 5% CO_2. The complete medium was replaced every 2 to 3 d.

2.7. In Vitro LIPUS Application

The pulsed ultrasound signal was transmitted at a frequency of 3 MHz with a spatially averaged intensity of 30 mW/cm^2 and a pulse rate of 1:4 (2 ms on and 8 ms off, Osteotron-D IV). Cells began to be treated with LIPUS 24 h after cell seeding. A six-well plate was held in place, and the transducers were applied such that they directly touched the cell-containing medium.[23,24] The distance between the transducer and the cells was less than 4 mm. The cell culture was exposed to a single treatment of ultrasound for 15 min.[25,26] Ultrasound treatment was performed with the culture dishes in an incubator (37 °C, 5% CO_2-95% air). Control samples were subjected to the same procedures under the same conditions but without ultrasound stimulation.

2.8. Count of Cell Number

MC3T3-E1 cells were seeded onto Ti and SS discs in six-well plates. Then, 2 × 10^4 cells were cultured with or without daily LIPUS stimulation for 1, 3 and 7 days. Cells in the four 1mm corner squares were counted by a hemocytometer under a light microscope. The total cell numbers were determined with the following calculation: Total cells = cell density (cells / ml) x original volume of sample (ml)

2.9. Determination of Alkaline Phosphatase (ALP) Activity

To measure the ALP activity, MC3T3-E1 cells were seeded onto Ti and SS discs in six-well dishes. Then, 2 × 10^4 cells were cultured in the presence (LIPUS group) or absence (Control group) of daily LIPUS stimulation for 7 or 14 days. ALP contents in the control and LIPUS groups were analyzed by the ALP kit (Wako), according to the manufacturer's instructions.

2.10. Determination of Mineralized Nodule Formation

MC3T3-E1 cells were seeded onto Ti and SS discs in six-well plates. Then, 2×10^4 cells were cultured with or without daily LIPUS stimulation for 21 days. The condition of the cells and presence of nodule formation were checked routinely under stereomicroscopy. The presence of mineralized nodules was determined by alizarin red (AR) staining (Wako).

2.11. Real-Time Polymerase Chain Reaction (PCR) Analysis

Cells were cultured with or without daily LIPUS stimulation for 7 days. All cultures were terminated 24 h after the last ultrasound exposure. Total RNA was extracted from each culture dish by using Trizol reagent according to the manufacturer's instructions. The mRNA was reverse-transcribed to yield cDNA, which served as a template for real-time PCR, to determine the expression level of osteogenic factors. For this purpose, a 7500 real-time PCR system and SYBR Green Master Mix (Applied Biosystems, Foster City, CA) were used. Real-time PCR was performed with the following cycle conditions: 2 min at 50 °C, 10 min at 95 °C, 40 cycles of 15 s at 95 °C, and 1 min at 60 °C. The primer pairs for the mouse genes are listed in Table 1. The PCR products were electrophoresed and quantified by scanning with an optical densitometer. Expression levels of all genes were normalized to the expression level of β-actin (as a housekeeping gene) within the same sample. Ratios of target genes to β-actin were calculated by a digital image analysis software (ImageJ).

2.12. Statistical Analysis

All data are presented as the mean ± standard deviation (SD). Mean differences between the groups were assessed with the Statistical Package for the Social Sciences (SPSS version 15; Chicago, IL) by one-way analysis of variance (ANOVA). Comparisons between the LIPUS and control groups

were performed using the Mann-Whitney U test. In all cases, differences were considered statistically significant at the 5% level of significance.

3. RESULTS

3.1. μ-CT Analysis

The CBD and CBT around Ti MSIs were enhanced on the LIPUS-treated side on days 7 and 14 ($P < 0.05$; Fig. 2(A) and Fig. 3(A) for CBD and CBT, respectively, Table 2). The CBR around Ti MSIs was higher on the LIPUS-treated side than on the control side on day 14 ($P < 0.05$, Fig. 4(A)). The CBD around the SS MSIs showed no differences between the LIPUS-treated and control sides from day 0 to day 7 after implantation, but the CBD was enhanced on the LIPUS-treated side on day 14 ($P < 0.05$, Fig. 2(B)). The CBT around the SS MSIs was increased by LIPUS application on day 14 ($P < 0.05$, Fig. 3(B)).The CBR around SS MSIs was higher on the LIPUS-treated side than on the control side on days 7 and 14 ($P < 0.05$, Fig. 4(B)).

3.2. SEM Analysis

The bone-implant contact (BIC) around the Ti MSIs was higher on the LIPUS-treated side compared to the control side on days 7 and 14 ($P < 0.05$, Fig. 5(A), Table 2). The BIC around the SS MSIs was enhanced by LIPUS application on day 14 ($P < 0.05$, Fig. 5(B)). There was no significant difference in BIC between the Ti and SS MSIs on day 3. However, on days 7 and 14, the Ti MSIs showed more BIC than the SS MSIs (Fig. 6).

3.3. In Vitro Bone Formation

The numbers of MC3T3-E1 cells were increased by LIPUS application on both Ti and SS discs on days 3 and 7 ($P < 0.05$, Fig. 7). For osteogenic cells on both Ti and SS discs, the ALP activity was enhanced by LIPUS stimulation for 14th d (Fig. 8). Mineralized nodule formation in the cells was detected after LIPUS stimulation for 21 d. The AR staining of mineralized nodules was more intense in the LIPUS-stimulated cells compared to the control cells, on both the Ti and SS discs (Fig. 9). Expression of ALP mRNA was significantly increased in osteogenic cells on both Ti and SS discs by 3 d after LIPUS application ($P < 0.05$, Fig. 10).

4. DISCUSSION

The purpose of the present study was to investigate whether LIPUS exposure could enhance bone formation around Ti and SS MSIs in *in vivo* and *in vitro* experiments. Bone formation on the LIPUS-treated side started earlier and became more extensive than bone formation on the control side. The findings of this study provide a new strategy for increasing the initial stability of MSIs after implantation. To the authors' knowledge, this study is the first to examine the effect of LIPUS exposure on bone formation around MSIs.

The BIC between the Ti MSI and surrounding bone was 23% ± 8% on day 7 and 38% ± 16% on day 14. For the SS MSI, these values were 20% ± 7% and 34.5% ± 13%, respectively. A previous report suggested that a BIC of 10–58% can successfully resist orthodontic loads.[27] In addition, the CBR increased gradually after the implantation of MSIs of either material from day 3 to day 14. Therefore, both types of MSIs might be suitable as orthodontic anchorage devices.

A limitation of the present study was the use of tibiae instead of maxillofacial bones. It is technically difficult to implant MSIs in the maxillofacial bones of rats and to confine the LIPUS energy to the experimental side. Most reports evaluating the effect of LIPUS on bone healing have

chosen tibiae for implantation sites.[28,29] However, two studies evaluated the BIC of Ti implants placed on the maxillofacial bone, reporting BIC values of 23.4% ± 17.9% to 33.9% ± 3.3%.[30,31] These values are similar to the present results, suggesting that there may not be a significant difference in BIC values obtained with tibiae versus maxillofacial bones.

To the best of the authors' knowledge, no study has evaluated the potential utility of LIPUS in promoting bone formation after SS MSI placement. 316L SS was chosen as a material for study because its composition, microstructure, and tensile properties are standardized in ISO and ASTM material specifications. The Ti and SS MSIs showed osseointegration with the surrounding bone *in vivo.* Bone formation and mineralization were promoted on the discs. With the increased demand for Ti and its use in various fields, this metal is becoming more expensive.[32] Moreover, a major concern in MSI usage is screw breakage during insertion or removal.[8] Using MSIs made of SS might reduce the possibility of screw breakage because SS is stronger than Ti-6Al-4V alloy.[33] Recent reports have suggested that SS MSIs could be used as temporary anchorage devices.[34,35] In previous reports, SS MSIs showed no significant differences from Ti MSIs in terms of stress distribution,[36] rate of screw failure until removal,[37] microdamage in the surrounding bones, rate of BIC,[35] or stability.[38] Moreover, SS MSIs had higher insertion torque values than Ti MSIs.[35] In terms of biocompatibility, Blaya et al.[39] found no significant difference in the metal ion concentration at different time points after 316L SS and Ti-6Al-4V MSI placement. There was no difference in infection rate between Ti and SS nails when used in the fixation of pediatric femoral fracture.[40] These findings suggest the possibility that SS MSIs can be used instead of Ti MSIs.

In this study, MC3T3-E1 cells were cultured on Ti and SS discs to compare effects of LIPUS application on bone cell metabolism. The cell numbers counted by hemocytometry were significantly increased by LIPUS stimulation on Ti and SS discs from day 3 to day 7. As a marker

of osteoblast differentiation, the ALP activity was higher on the LIPUS-treated discs than on the control discs 2 weeks after LIPUS application. These results suggest that LIPUS application might induce the differentiation of osteogenic cells in vitro. LIPUS stimulation also increased the formation of mineralized nodules in osteoblastic cells 3 weeks after application, which was evident by the intensity of AR staining. Additionally, expression of ALP mRNA was increased on both Ti and SS discs after 3 d of LIPUS stimulation. This result indicates that LIPUS can promote not only the differentiation, but also the mineralization, of osteoblasts on Ti and SS discs.

One of the most desirable properties in the clinical usage of metallic implants is to achieve osseointegration onto the surrounding bones as quickly as possible. In addition to its role in orthodontics, this property has great benefit in orthopedics because it can allow early fixation during bone healing in reconstructive surgery or artificial joint replacement. LIPUS application significantly increased the BIC around both metallic implants, enhanced the CBD, CBT, and CBR results after implantation, and increased the number of osteogenic cells on the metallic discs. Together, these findings demonstrate the efficiency of LIPUS in bone formation. Therefore, LIPUS might be useful for enhancing osseointegration after implantation and tissue engineering around both Ti and SS implants.

5. CONCLUSIONS

The results of this study suggest that LIPUS application enhances bone formation around both Ti and SS MSIs. Therefore, LIPUS exposure might enhance the initial stability and improve the success rate of MSIs.

ACKNOWLEDGEMENT

We are grateful to Nobuyasu Yamanaka and Atsushi Chuma for providing the ultrasound devices and technical support for the experiments. This study was supported by Grants-in-Aid for Scientific Research from the Ministry of Education, Culture, Sports, Science, and Technology of Japan (No. 25463185). The authors declare no potential conflicts of interest with respect to the authorship and/or publication of this article.

REFERENCE

1. Roberts WE, Helm FR, Marshall KJ, Gongloff RK. Rigid endosseous implants for orthodontic and orthopedic anchorage. *Angle Orthod* 1989; 59: 247–56.
2. Creekmore TD, Eklund MK. The possibility of skeletal anchorage. *J Clin Orthod* 1983; 17:266–9.
3. Umemori M, Sugawara J, Mitani H, Nagasaka H, Kawamura H. Skeletal anchorage system for open-bite correction. *Am J Orthod Dentofacial Orthop* 1999; 115: 166-74.
4. Park HS, Bae SM, Kyung HM, Sung JH. Micro-implant anchorage for treatment of skeletal Class I bialveolar protrusion. *J Clin Orthod* 2001; 35:417–22.
5. Kuroda S, Katayama A, Takano-Yamamoto T. Severe anterior open-bite case treated using titanium screw anchorage. *Angle Orthod* 2004; 74:558–67.
6. Kyung HM, Park HS, Bae SM, Sung JH, Kim IB. Development of orthodontic micro-implants for intraoral anchorage. *J Clin Orthod* 2003; 37:321–8.
7. Kuroda S, Sugawara Y, Deguchi T, Kyung HM, Takano-Yamamoto T. Clinical use of miniscrew implants as orthodontic anchorage: Success rates and postoperative discomfort. *Am J Orthod Dentofacial Orthop* 2007;131: 9–15.
8. Kravitz ND, Kusnoto B. Risks and complications of orthodontic miniscrews. *Am J Orthod Dentofacial Orthop* 2007; 131:S43–51.
9. Papageorgiou SN, Zogakis IP, Papadopoulos MA. Failure rates and associated risk factors of orthodontic miniscrew implants: A meta-analysis. *Am J Orthod Dentofacial* 2012; 142:577–95,

10. Waden SJ, Bennell KL, McMeeken JM, Wark JD. Acceleration of fresh fracture repair using the sonic accelerated fracture healing system (SAFHS): A review. *Calcif Tissue Int* 2000; 66:157–63.
11. Azuma Y, Ito M, Harada Y, Takagi H, Ohta T, Jingushi S. Low-intensity pulsed ultrasound accelerates rat femoral fracture healing by acting on the various cellular reactions in the fracture callus. *J Bone Miner Res* 2001; 16: 671–80.
12. Angle SR, Sena K, Sumner DR, Virdi AS. Osteogenic differentiation of rat bone marrow stromal cells by various intensities of low-intensity pulsed ultrasound. *Ultrasonics* 2011; 51:281–8.
13. Takikawa S, Matsui N, Kokubu T, Tsunoda M, Fujioka H, Mizuno K, Azuma Y. Low-intensity pulsed ultrasound initiates bone healing in rat nonunion fracture model. *J Ultrasound Med* 2001; 20:197–205.
14. Pipi E. Bossini FP, Oliveira P, Ribeiro JU, Tim C, Parizotto NA, Alves JM, Ribeiro DA, Araujo HSS, Renno ACM. Low-intensity pulsed ultrasound produced an increase of osteogenic genes expression during the process of bone healing in rats. *Ultrasound Med Biol* 2010; 36:2057–64.
15. Busse JW, Bhandari M, Kulkarni AV, Tunks E. The effect of low intensity pulsed ultrasound therapy on time to fracture healing: A meta-analysis. *Can Med Assoc J* 2002; 166: 437–41.
16. Shakouri K, Eftekharsadat B, Oskuie MR, Soleimanpour J, Tarzamni MK, Salekzamani Y, Hoshyar Y, Nezami N. Effect of low-intensity pulsed ultrasound on fracture callus mineral density and flexural strength in rabbit tibial fresh fracture. *J Orthop Sci* 2010; 15: 240–4.

17. Parvizi J, Wu CC, Lewallen DG, Greenleaf JF, Bolander ME. Low-intensity ultrasound stimulates proteoglycan synthesis in rat chondrocytes by increasing aggrecan gene expression. *J Orthop Res* 1999; 17:488–94.
18. Yang KH, Parvizi J, Wang SJ, Lewallen GD, Kinnick RR, Greenleaf JF, Bolander ME. Exposure to low-intensity ultrasound increases aggrecan gene expression in a rat femur fracture model. *J Orthop Res* 1996; 14:802–9.
19. Wijdicks CA, Virdi AS, Sena K, Sumner DR, Leven RM. Ultrasound enhances recombinant human bmp-2 induced ectopic bone formation in a rat model. *Ultrasound Med Biol* 2009; 35: 1629–37.
20. Pounder NM, Harrison AJ. Low intensity pulsed ultrasound for fracture healing: A review of the clinical evidence and the associated biological mechanism of action. *Ultrasonics* 2008; 48:330–8.
21. Lim K, Kim J, Seonwoo H, Park SH, Choung PH, Chung JH. In vitro effects of low-intensity pulsed ultrasound stimulation on the osteogenic differentiation of human alveolar bone-derived mesenchymal stem cells for tooth tissue engineering. *BioMed Res Int* 2013; 1-15.
22. Unsworth J, Kaneez S, Harris S, Ridgway J, Fenwick S, Chenery D, Harrison A. Pulsed low intensity ultrasound enhances mineralization in preosteoblast cells. *Ultrasound Med Biol* 2007; 33:1468–74.
23. Katiyar A, Duncan RL, Sarkar K. Ultrasound stimulation increases proliferation of MC3T3-E1 preosteoblast-like cells. *J Ther Ultrasound* 2014; 2:1-10.
24. Reher P, Harris M, Whiteman M, Hai HK, Meghji S. Ultrasound stimulates nitric oxide and prostaglandin E2 production by human osteoblasts. *Bone* 2002; 31:236–41.

25. Inubushi T, Tanaka E, Rego EB, Ohtani A, Kawazoe A, Tanne K, Miyauchi M, Takata T. Ultrasound stimulation attenuates resorption of tooth induced by experimental force application. Bone 2013; 53: 497–506.
26. Nagata K, Nakamura T, Fujihara S, Tanaka E. Ultrasound modulates the inflammatory response and promotes muscle regeneration in injured muscles. *Ann Biomed Eng* 2013; 41:1095-105.
27. Cornelis MA, Scheffler NR, Clerck HJ, Tulloch JF, Behets CN. Systematic review of the experimental use of temporary skeletal anchorage devices in orthodontics. *Am J Orthod Dentofacial Orthop* 2007; 131:S52–8.
28. Ustun Y, Erdogan O, Kurkcu M, Akova T, Damlar I. Effect of low intensity pulsed ultrasound on dental implant osseointegration: A preliminary report. *Eur J Dent* 2008; 2: 254–62.
29. Liu Q, Liu X, Liu B, Hu K, Zhou X, Ding Y. The effect of low-intensity pulsed ultrasound on the osseointegration of titanium dental implants. *Brit J Oral Maxillofac Surg* 2012; 50:244–50.
30. Deguchi T, Takano-Yamamoto T, Kanomi T, Hartsfield JK, Roberts WE, Garetto LP. The use of small titanium screws for orthodontic anchorage. *J Dent Res* 2003; 82:377–81.
31. Kim JW, Ahn SJ, Chang YI. Histomorphometric and mechanical analyses of the drill-free screw as orthodontic anchorage. Am J Orthod dentofacial Orthop 2005; 128:190–4.
32. Lim YW, Kwon SY, Sun DH, Kim YS. Enhanced biocompatibility of stainless steel implants by titanium coating and microarc oxidation. *Clin Orthop Relate Res* 2011; 469: 330–8.

33. Chen PQ, Lin SJ, Wu SS, So H. Mechanical performance of the new posterior spinal implant: effect of materials, connecting plate, and pedicle screw design. *Spine* 2003; 28: 881–6.
34. Basha AG, Shantaraj R, Morgegowda SB. Comparative study between conventional en-masse retraction (sliding mechanics) and en-masse retraction using orthodontic micro implant. *Implant dent* 2010; 19: 128–36.
35. Brown RN, Sexton BE, Chu TMG, Katona TR, Stewart KT, Kyung HM, Liu SSY. Comparison of stainless steel and titanium alloy orthodontic miniscrew implants: A mechanical and histologic analysis. *Am J Orthod Dentofacial Orthop* 2014; 145: 496–505.
36. Singh S, Mogra S, Shetty VS, Shetty S, Philip P. Three-dimensional finite element analysis of strength, stability, and stress distribution in orthodontic anchorage: A conical, self-drilling miniscrew implant system. *Am J Orthod Dentofacial Orthop* 2012; 141:327–36.
37. Bachoura A, Yoshida R, Lattermann C, Kamineni S. Late removal of titanium hardware from the elbow is problematic. *ISRN Orthop* 2012; 2012:1-4.
38. Lan H, Liu PH, Chang HP. Influence of different implant materials on the primary stability of orthodontic mini-implants. *Kaohsiung J Mel Sci* 2012; 28:673–8.
39. Blaya MG, Blaya DS, Mello P, Flores EMM, Hirakata LM. Titanium alloy miniscrews for orthodontic anchorage: an in vivo study of metal ion release. *J Dent Sci* 2011; 26:209–14.
40. Wall EJ, Jain V, Vora V, Mehlman CT, Crawford AH. Complications of titanium and stainless steel elastic nail fixation of pediatric femoral fractures. *J Bone and Joint Surg Am* 2008; 90:1305–13.

FIGURE LEGENDS

Figure 1: SEM images of Ti MSIs. (A) Representative images of experimental implants after 14 days of LIPUS exposure. (B) Regions of interest for BIC measurements were calculated by digital image analysis software. MSI contact ratio (%) = (Length of bone contact/length of MSI surface) × 100. All measurements were calculated under 200× magnification. (C) SEM micrographs of implant surface. Boxed areas are enlarged to right. The arrow leading to BIC.

Figure 2: CBD values around the Ti (A) and SS (B) MSIs, without (CTRL) or with (LPS) LIPUS application. *$P < 0.05$.

Figure 3: CBT values around the Ti (A) and SS (B) MSIs, without (CTRL) or with (LPS) LIPUS application. *$P < 0.05$.

Figure 4: CBR values with the Ti (A) and SS (B) MSIs, without (CTRL) or with (LPS) LIPUS application. *$P < 0.05$.

Figure 5: BIC around the Ti (A) and SS (B) MSIs, without (Control) or with LIPUS application. *$P < 0.05$.

Figure 6: SEM images of MSIs after 14 days of implantation: (A) Ti MSI with LIPUS application, (B) Ti MSI without LIPUS application (CTRL), (C) SS MSI with LIPUS application, and (D) SS MSIs without LIPUS applications (CTRL). Scale bar: 500 μm.

Figure 7: Numbers of MC3T3-E1 cells on the Ti (A) and SS (B) discs, without (Control) or with LIPUS application. *$P < 0.05$, **$P < 0.01$.

Figure 8: ALP staining of MC3T3-E1 cells cultured on Ti and SS discs after 2 weeks of culture, without (Ti: A, SS: C) or with (Ti: B, SS: D) LIPUS application. Boxed areas are enlarged to the right. Scale bars: 1,000 μm.

Figure 9: Osteoblast mineralization observed by AR staining of MC3T3-E1 cells on Ti and SS discs after 3 weeks of culture, without (Ti: A, SS: C) or with (Ti: B, SS: D) LIPUS application. Red region indicates calcium deposition. Boxed areas are enlarged to the right. Scale bars: 1000 μm.

Figure 10: Expression of ALP mRNA in MC3T3-E1 cells cultured on Ti (A) and SS (B) discs without (Control) or with LIPUS application. *$P < 0.05$.

Table 1 RT-PCR primer sequences used in the RT- PCR experiments

Target gene	Annealing T (°C)	Sequence	
ALP	60	Forward:	GGG TTT CGG TTG GCA TCA TA
		Reverse:	AAC TCA CCT CAT GGG CCT CTT
B-actin	58	Forward:	GCT CTT TTC CAG CCT TCC TT
		Reverse:	AGG TCT TTA CGG ATG TCA ACG

ALP: Alkaline phosphatase

Table 2: Measurements in μ-CT and SEM analyses

	Ti			SS		
	LIPUS	Control	P-value	LIPUS	Control	P-value
Day0						
CBD (mg/cm^3)	13.79±0.15	13.79±0.21	N.S.	16.05±0.1	16.05±0.13	N.S.
CBT (mm)	0.18±0.05	0.18±0.06	N.S.	0.15±0.12	0.15±0.08	N.S.
CBR (%)	61.0±11.77	61.0±11.77	N.S.	59.6±4.23	59.6±4.23	N.S.
BIC (%)	6.2±0.83	6.2±0.83	N.S.	5.7±0.92	5.7±0.92	N.S.
Day3						
CBD (mg/cm^3)	17.38±0.28	16.33±0.23	N.S.	19.08±0.19	18.74±0.24	N.S.
CBT (mm)	0.23±0.02	0.22±0.021	N.S.	0.19±0.18	0.19±0.16	N.S.
CBR (%)	67.9±3.69	62.9±3.42	N.S.	73.3±3.00	71.9±10.63	N.S.
BIC (%)	14.5±1.7	11.7±1.91	N.S.	15.7±3.10	12.5±2.06	N.S.
Day7						
CBD (mg/cm^3)	18.37±0.25	17.16±0.29	p<0.05	19.09±0.21	18.92±0.31	N.S.
CBT (mm)	0.25±0.09	0.22±0.1	p<0.05	0.2±0.16	0.19±0.23	N.S.
CBR (%)	69.6±7.05	65.5±6.23	N.S.	78.7±1.29	74.0±5.74	p<0.05
BIC (%)	31.5±2.5	23.0±2.62	p<0.05	26.5±2.5	20.2±2.62	p<0.05
Day14						
CBD (mg/cm^3)	19.35±0.25	17.32±0.27	p<0.05	25.27±0.28	23.4±0.23	p<0.05
CBT (mm)	0.28±0.12	0.23±0.09	p<0.05	0.23±0.13	0.21±0.16	p<0.05
CBR (%)	70.1±3.69	65.5±2.36	p<0.05	79.6±2.02	75.0±4.75	p<0.05
BIC (%)	54.7±2.08	38.2±1.41	p<0.05	47.5±2.08	34.5±1.41	p<0.05

All values are mean ± standard deviation (SD). Cortical bone density (CBD), cortical bone thickness (CBT), cortical bone rate (CBR) and bone implant contact (BIC) were measured. N.S. not significant, p<0.05 comparisons between the LIPUS and control groups were performed with the Mann-Whitney U test.

Figure 1

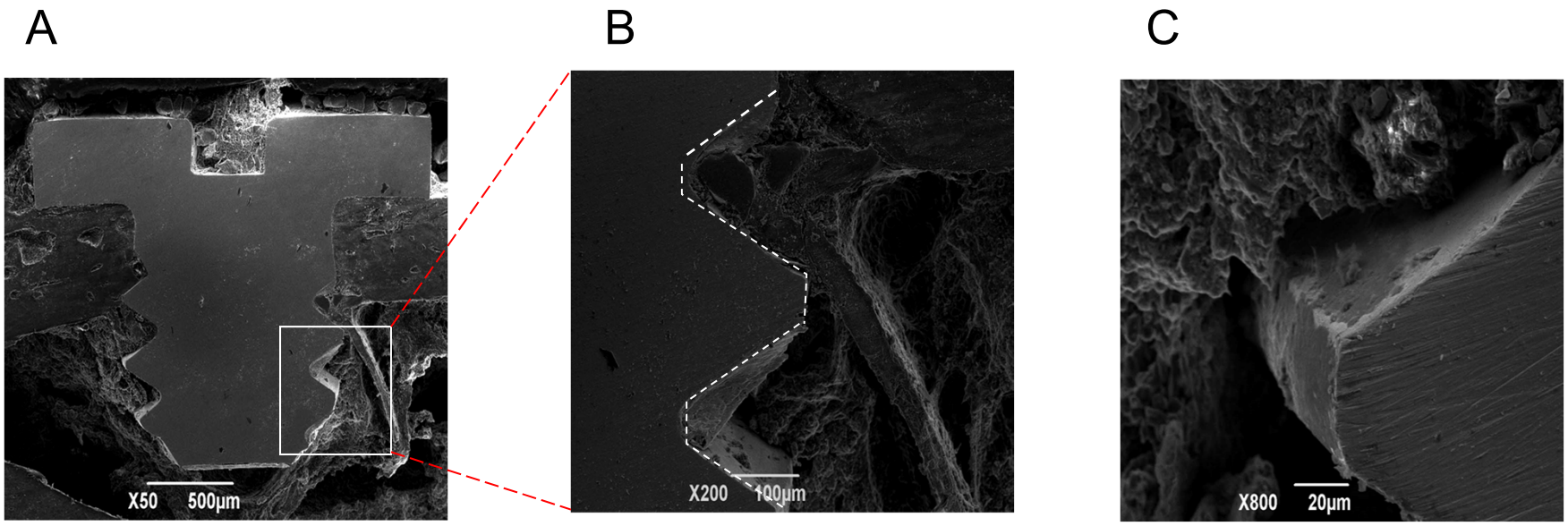

Figure 2

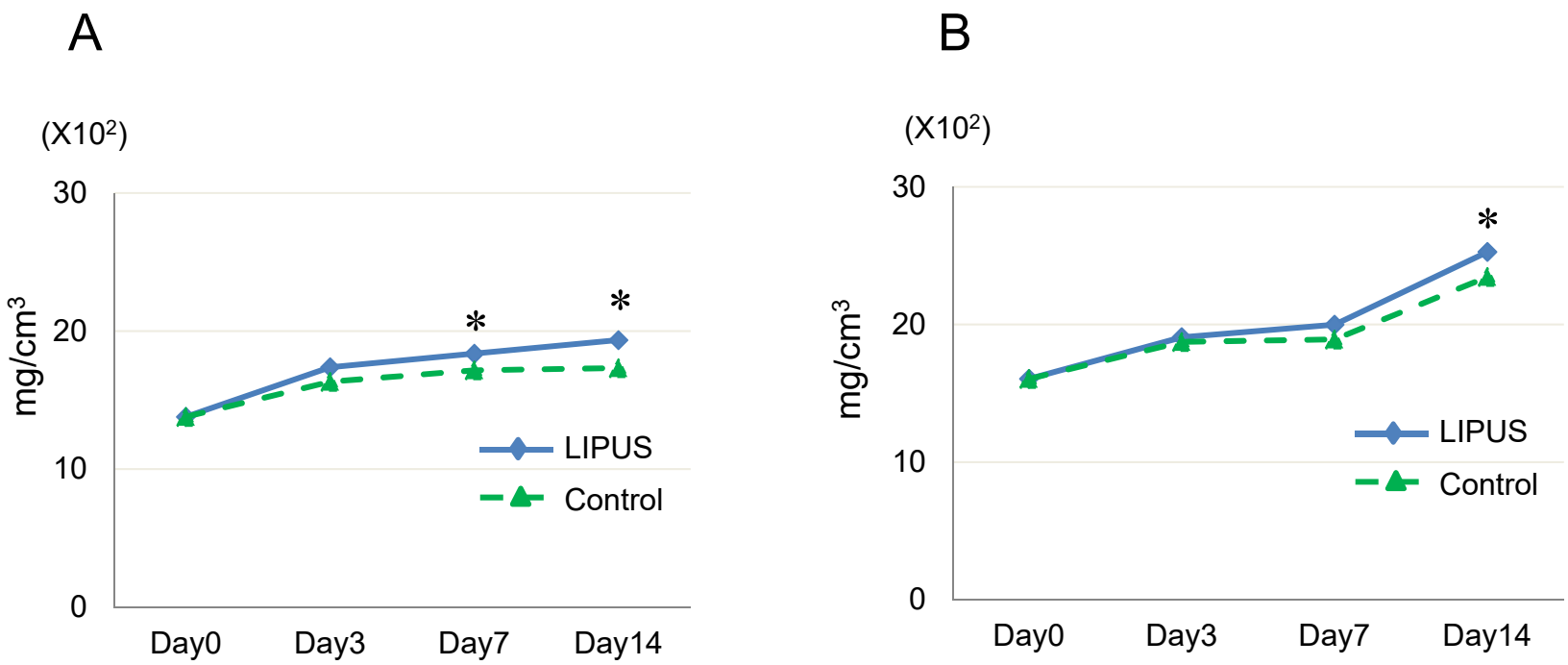
A
(X10²)
30
20
10
0
mg/cm³
*
*
LIPUS
Control
Day0
Day3
Day7
Day14
B
(X10²)
30
20
10
0
mg/cm³
*
LIPUS
Control
Day0
Day3
Day7
Day14

Figure 3

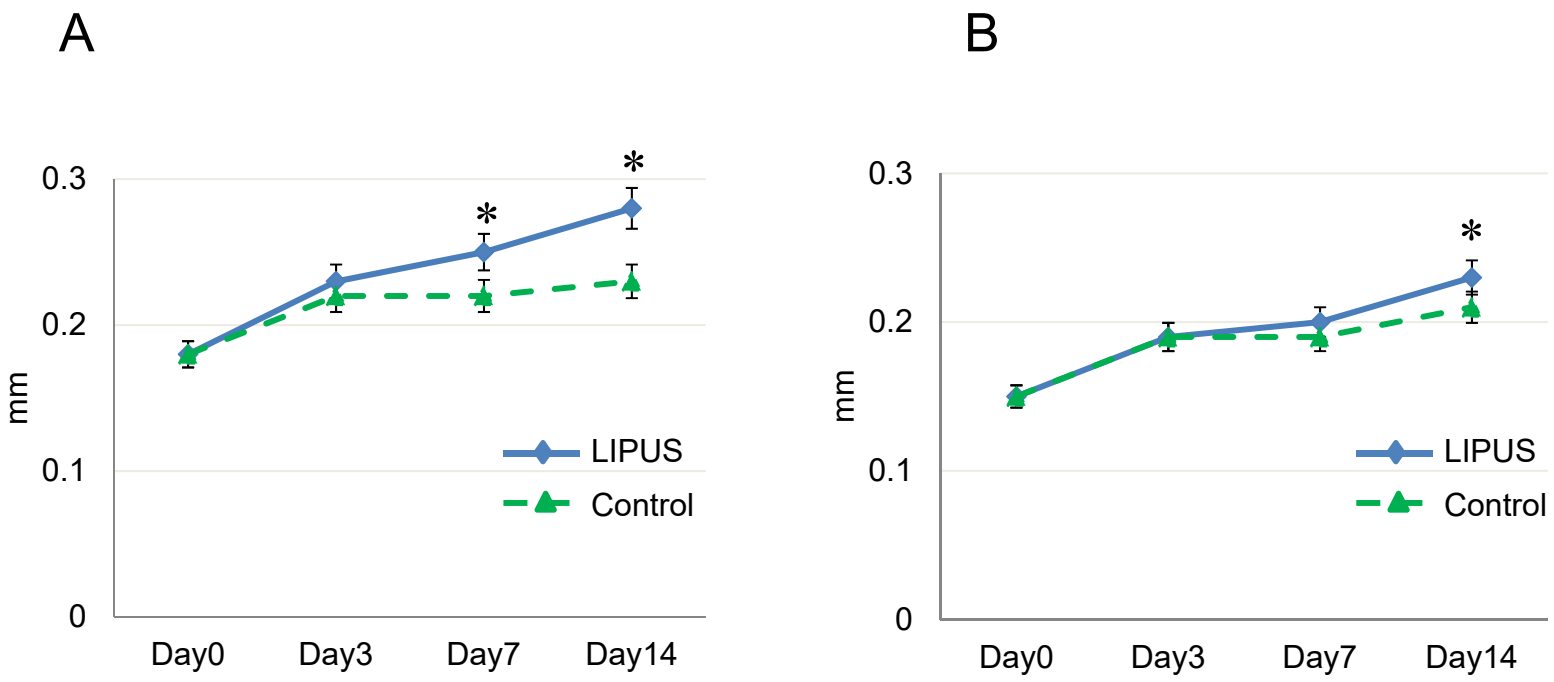

Figure 4

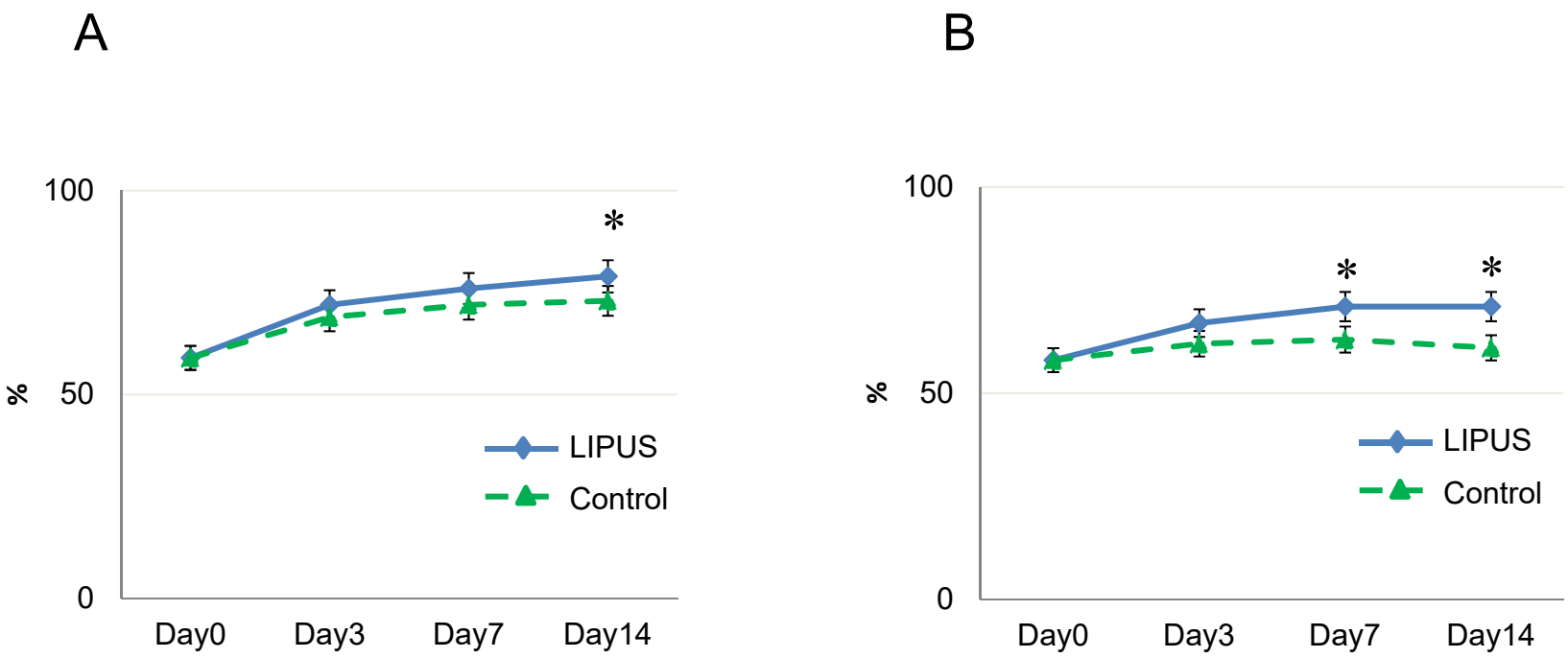
A
100
50
0
%
*
LIPUS
Control
Day0
Day3
Day7
Day14
B
100
50
0
%
*
*
LIPUS
Control
Day0
Day3
Day7
Day14

Figure 5

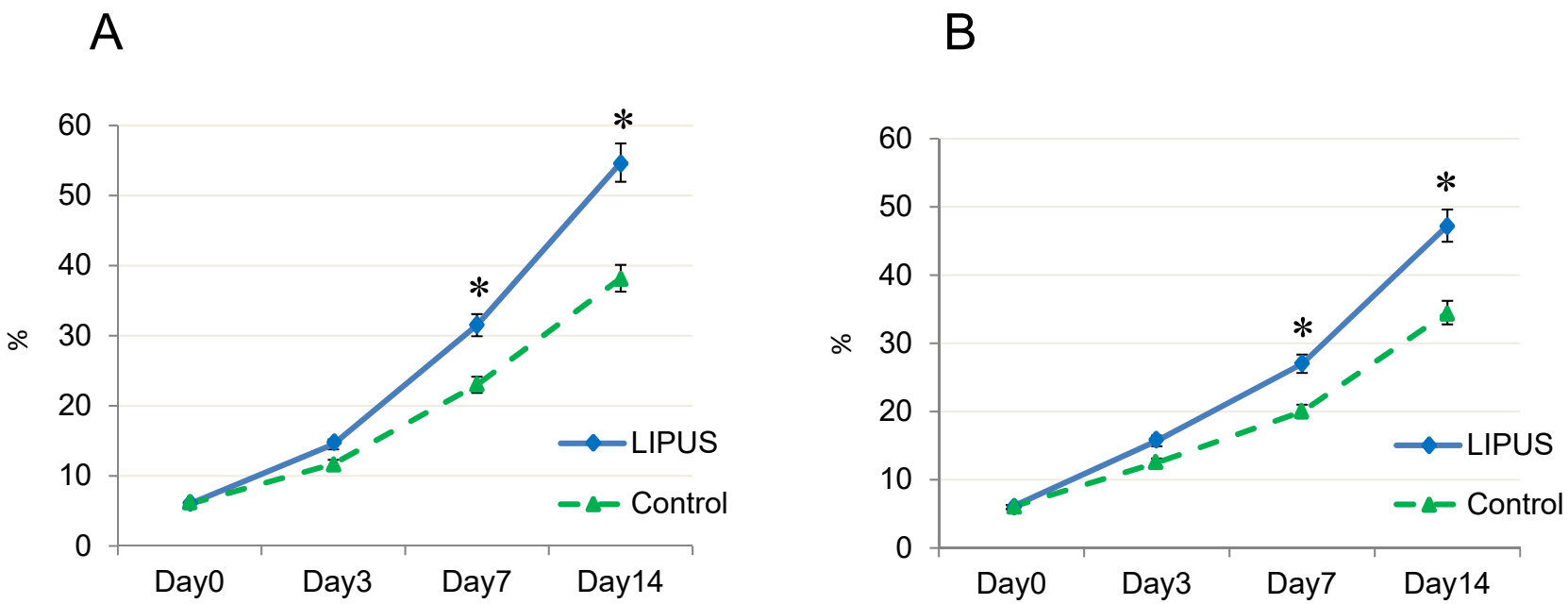

Figure 6

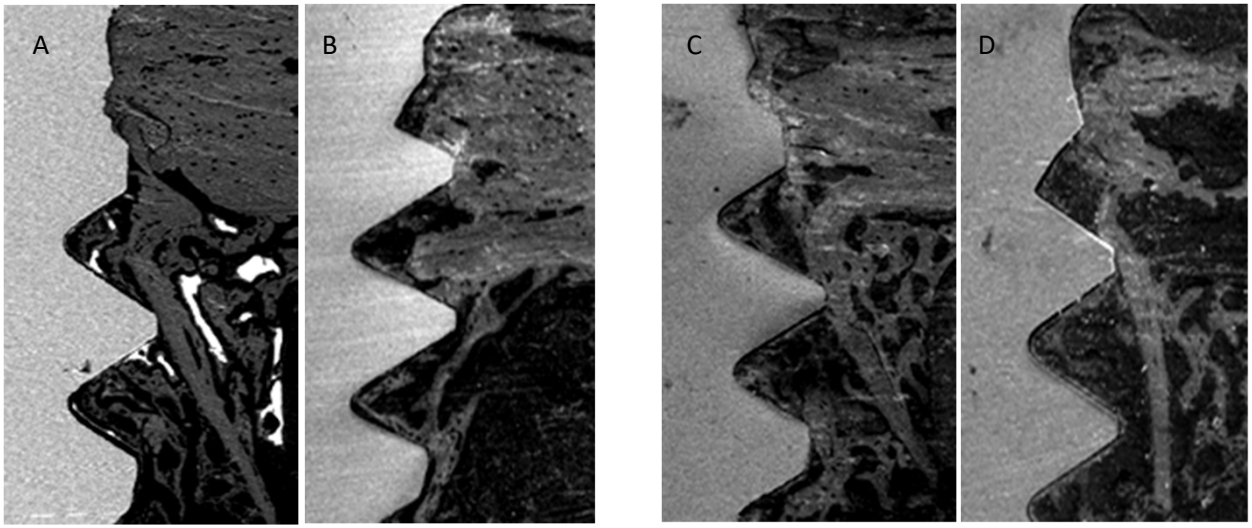

Figure 7

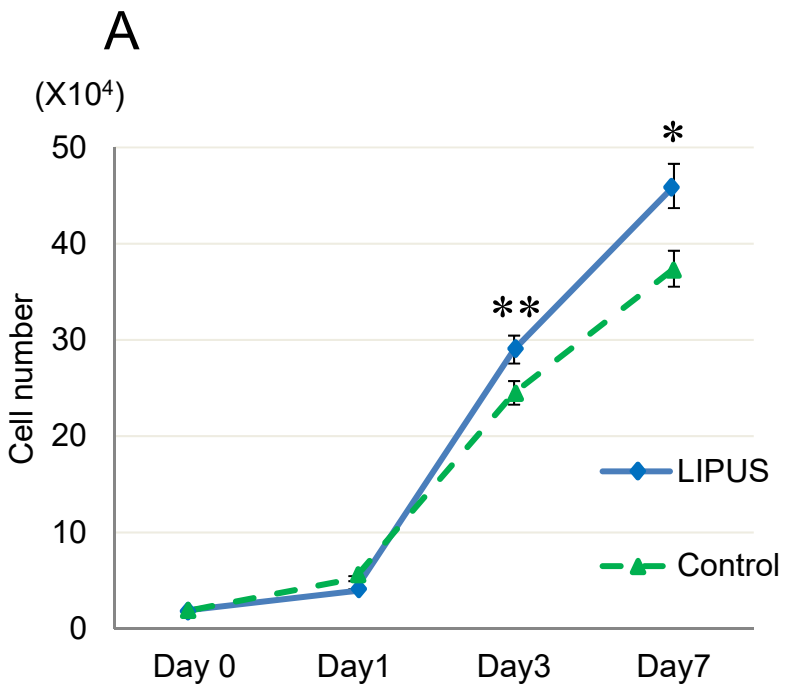
A
(X10⁴)
Cell number
50
40
30
20
10
0
*
**
LIPUS
Control
Day 0
Day1
Day3
Day7

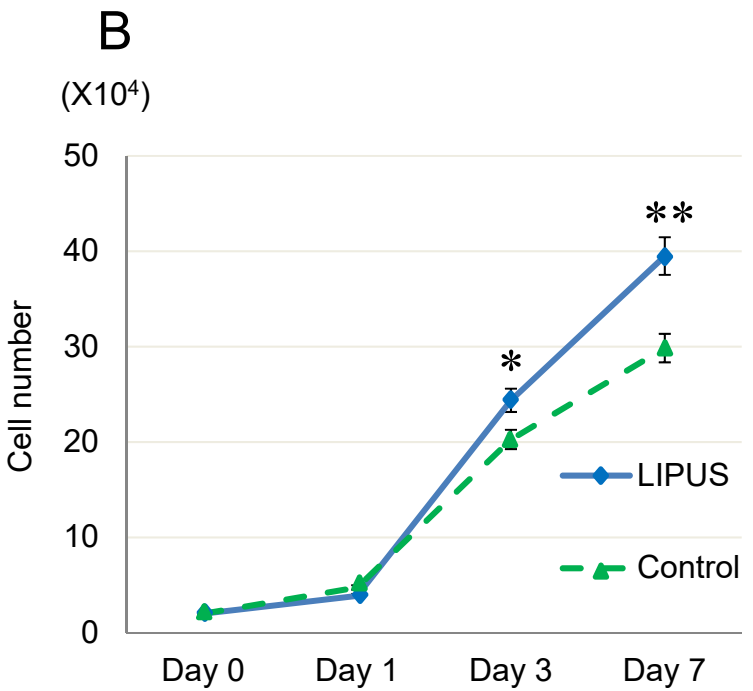
B
(X10⁴)
Cell number
50
40
30
20
10
0
*
**
LIPUS
Control
Day 0
Day 1
Day 3
Day 7

Figure 8

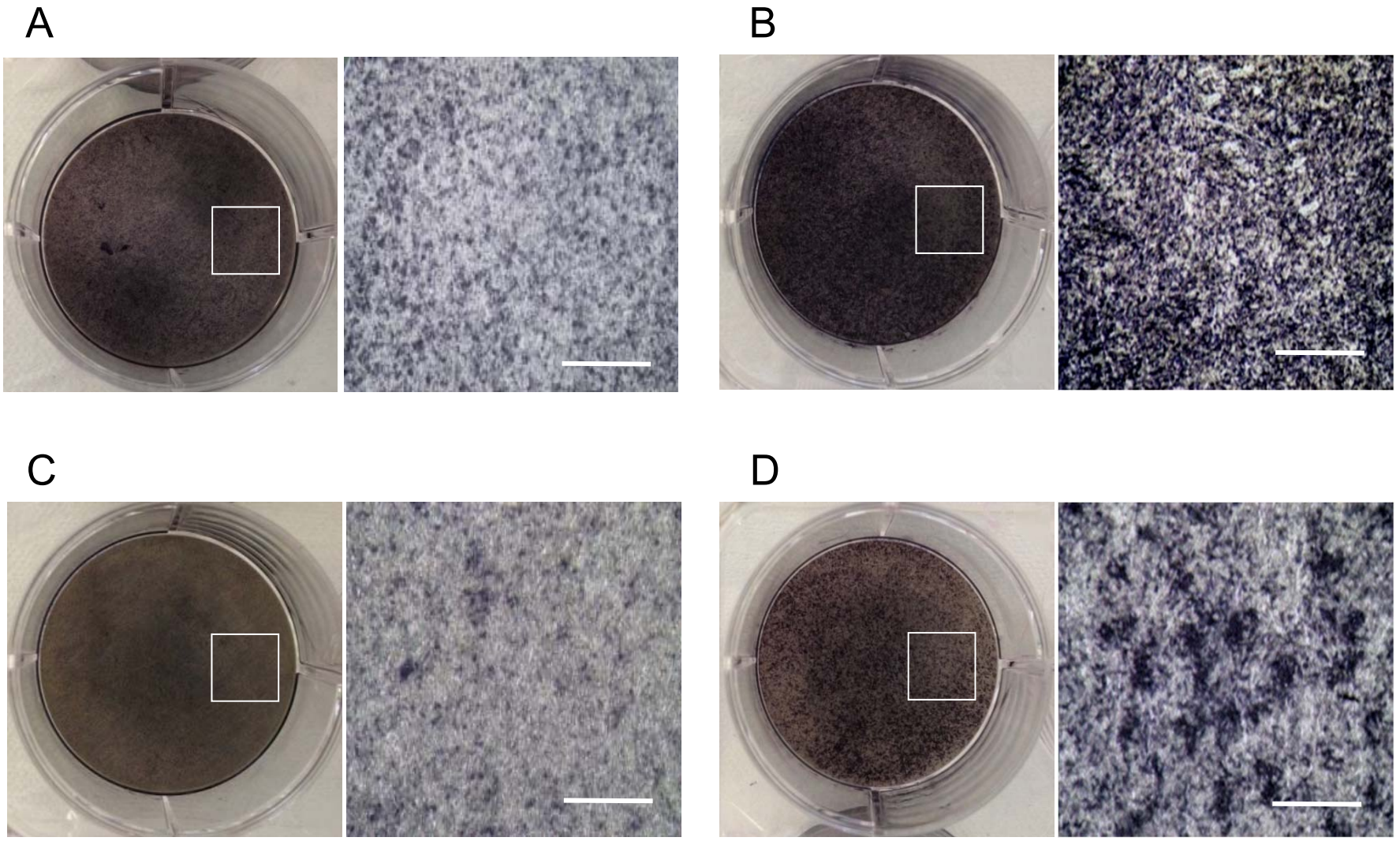

Figure 9

A

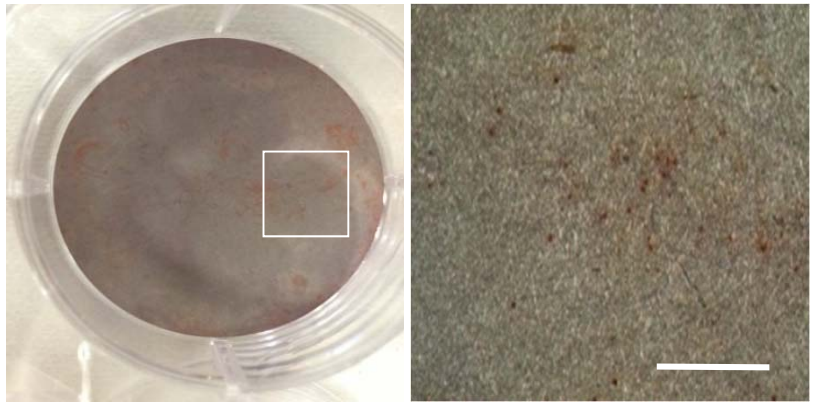

B

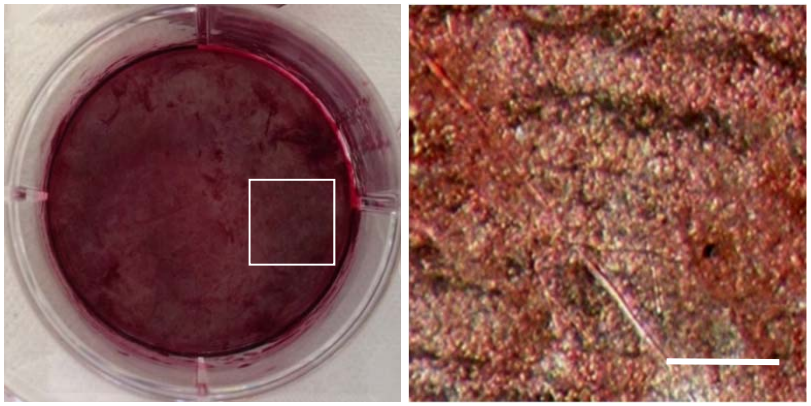

C

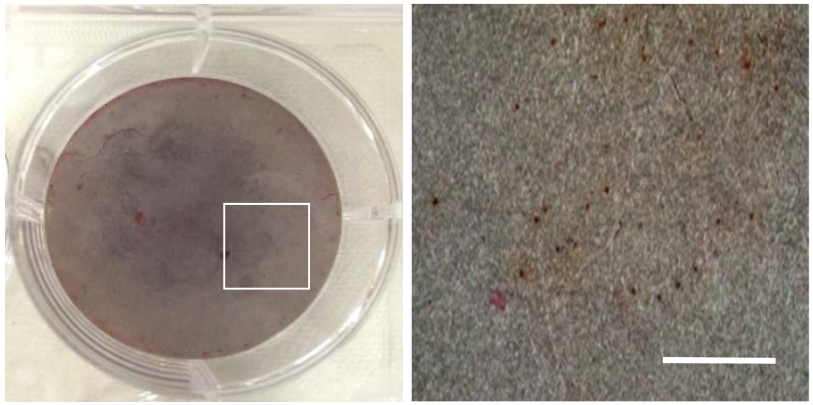

D

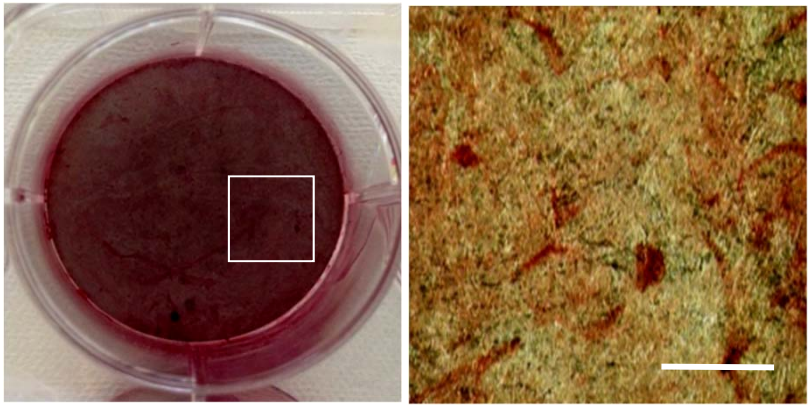

Figure 10

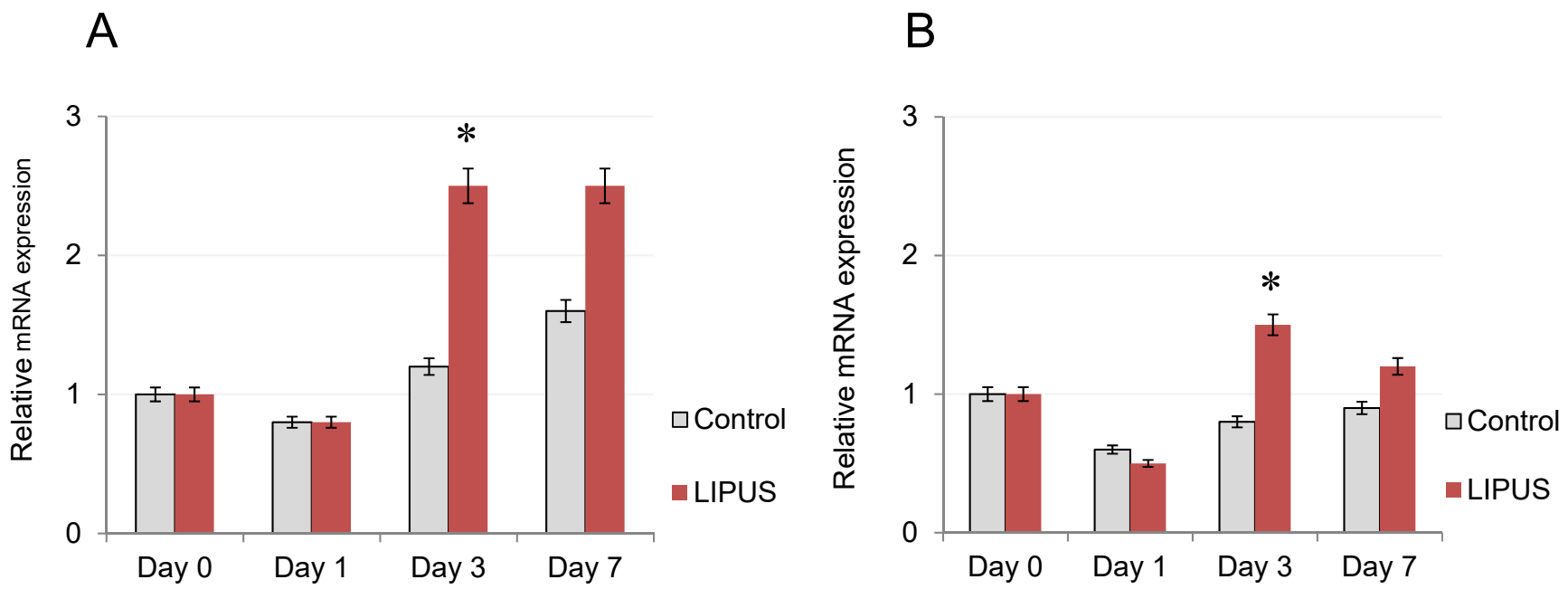
A
Relative mRNA expression
3
2
1
0
*
Day 0
Day 1
Day 3
Day 7
Control
LIPUS
B
Relative mRNA expression
3
2
1
0
*
Day 0
Day 1
Day 3
Day 7
Control
LIPUS